Published in Journal of Quantitative Spectroscopy and Radiative Transfer 221 (2018) 273 - 285

Co-Polarized and Cross-Polarized Scattering of an Off-Axis Focused Gaussian Beam by a Spherical Particle. 2. Sum Over Azimuthal Modes

James A. Lock[1,*] and Philip Laven[2]
[1]Physics Dept., Cleveland State University, Cleveland, OH 44115, USA
[2]9 Russells Crescent, Horley RH6 7DJ, UK
[*]Corresponding author. *E-mail address:* j.lock@csuohio.edu

Abstract
In static and dynamic light scattering, it has frequently been claimed that cross-polarized scattering cannot occur for single-scattering by a homogeneous spherical particle. Although this is true for both plane wave and on-axis Gaussian beam incidence, it does occur when the beam is translated off-axis incidence perpendicular to the scattering plane. An approximation to the co-polarized and cross-polarized scattering amplitudes is developed for which the sums over azimuthal modes can be evaluated analytically. This approximation provides a close fit to the exact generalized Lorenz-Mie polarization-resolved intensity for a number of off-axis locations of the incident beam.

Key words: Mie theory, generalized Lorenz-Mie theory, polarization-resolved scattering, cross-polarized scattering

1. Introduction

Part 1 of this study [1] dealt with a laser beam traveling in the horizontal +z direction that is linearly polarized either in the x direction perpendicular to the horizontal yz scattering plane (i.e. vertically or V) or in the scattering plane (i.e. horizontally or H), and is incident on a liquid-filled sample cell containing a large number of suspended spherical particles. Singly-scattered light passes through a polarizer oriented either vertically (V) or horizontally (H) before being recorded by a detector. If the incident beam is a plane wave, an on-axis focused Gaussian beam, or a Gaussian beam translated off-axis in the scattering plane, co-polarized VV and HH scattering will be observed but cross-polarized VH and HV scattering cannot occur. On the other hand, if the beam is translated off-axis with respect to a scattering particle in the direction perpendicular to the scattering plane, then both co-polarized and crossed-polarized scattering occur.

The body of this study proceeds as follows. The generalized Lorenz-Mie theory (GLMT) formulas for scattering of an off-axis localized model focused Gaussian beam by a spherical particle are reviewed in Section 2. The GLMT scattering amplitudes for off-axis beam incidence contain a sum over both partial waves n and azimuthal modes m. In Sections 3 and 4 the GLMT angular functions are expanded as an asymptotic series for large partial waves and for scattering angles away from 0° and 180°. The form of the individual terms of the asymptotic series allows the sum over azimuthal modes to be evaluated analytically, leaving only the sum over partial waves to be evaluated numerically, as is the case for Lorenz-Mie scattering of a plane wave. The predictions of the approximation are numerically compared with the results of the exact GLMT calculation. In Section 5, a similar approximation is derived for scattering angles near 0° and 180°. Our final conclusions concerning the approximation developed here are presented in Section 6. Lastly, an appendix gives a derivation of the far-zone diffracted electric field of an off-axis Gaussian beam by a circular aperture and its relation to the near-forward scattering amplitudes of Sec.5. The physical interpretation of the near-forward diffraction structure, the Debye series decomposition of the co-polarized and cross-polarized scattering amplitudes, and time-domain scattering of an off-axis Gaussian beam are presented in [2].

2. Off-Axis Scattering by a Focused Gaussian Beam

For convenience, this section repeats our main results for scattering of an off-axis localized model focused Gaussian beam by a spherical particle presented in [1]. The incident beam has the nominal electric field strength E_0, wavelength λ, wave number $k=2\pi/\lambda$, angular frequency ω, implicit time dependence $\exp(-i\omega t)$, and confinement parameter

$$s = \lambda/(2\pi w_0) \ . \tag{1}$$

The electric field half-width of the beam is w_0 and the center of the beam's focal waist is located at (ρ_0,φ_0) in a coordinate system in the $z=0$ plane whose origin coincides with the center of the scattering particle. The spherical particle has radius a and refractive index M.

The $r\rightarrow\infty$ far-zone scattered electric and magnetic fields are

$$\mathbf{E_{scatt}}(r,\theta,\varphi) = (iE_0/kr)\exp(ikr)\,[S_2(\theta,\varphi)\,\mathbf{u_\theta} - S_1(\theta,\varphi)\,\mathbf{u_\varphi}] \tag{2a}$$

$$\mathbf{B_{scatt}}(r,\theta,\varphi) = (iE_0/ckr)\exp(ikr)\,[S_1(\theta,\varphi)\,\mathbf{u_\theta} + S_2(\theta,\varphi)\,\mathbf{u_\varphi}] \ , \tag{2b}$$

where φ is the azimuthal angle of the scattering plane with respect to the xz plane, θ is the scattering angle in that plane, and c is the speed of light. The orthogonal unit vectors $\mathbf{u_r}$ and $\mathbf{u_\theta}$ lie in the scattering plane, and $\mathbf{u_\varphi}$ is perpendicular to it. The transverse magnetic (TM) and transverse electric (TE) partial wave scattering amplitudes of Lorenz-Mie theory are a_n, b_n, respectively, and the GLMT angular functions are

$$m\pi_n^{\,m}(\theta) = [m/\sin(\theta)]\,P_n^{\,m}[\cos(\theta)] \tag{3a}$$

$$\tau_n^{\,m}(\theta) = dP_n^{\,m}[\cos(\theta)]\,/\,d\theta \ , \tag{3b}$$

where $P_n^{\,m}[\cos(\theta)]$ are associated Legendre functions as defined in Eqs.(12.81),(12.81a) of [3].

If the electric field of the incident localized model Gaussian beam is x-polarized at the center of its focal waist, the GLMT scattering amplitudes are

$$\begin{aligned} S_1(\theta,\varphi;\rho_0,\varphi_0) = {} & i\sum_{n=1}^{\infty} c_n F_n (n+1/2)\, b_n\, I_1(Q_n)\, \tau_n^{\,0}(\theta)\, \sin(\varphi_0) \\ & + i\sum_{n=1}^{\infty} c_n F_n (n+1/2)\, b_n \sum_{m=1}^{n} [-i/(n+1/2)]^m\, \tau_n^{\,m}(\theta) \\ & \times [I_m^{-}(Q_n)\sin(m\chi)\cos(\varphi_0) + I_m^{+}(Q_n)\cos(m\chi)\sin(\varphi_0)] \\ & + i\sum_{n=1}^{\infty} c_n F_n (n+1/2)\, a_n \sum_{m=1}^{n} [-i/(n+1/2)]^m\, m\pi_n^{\,m}(\theta) \\ & \times [I_m^{+}(Q_n)\sin(m\chi)\cos(\varphi_0) + I_m^{-}(Q_n)\cos(m\chi)\sin(\varphi_0)] \end{aligned} \tag{4a}$$

and

$$S_2(\theta,\varphi;\rho_0,\varphi_0) = \mathrm{i}\sum_{n=1}^{\infty} c_n F_n (n+1/2)\, a_n \mathrm{I}_1(Q_n)\, \tau_n^0(\theta) \cos(\varphi_0)$$

$$+ \mathrm{i}\sum_{n=1}^{\infty} c_n F_n (n+1/2)\, a_n \sum_{m=1}^{n} [-\mathrm{i}/(n+1/2)]^m\, \tau_n^m(\theta)$$

$$\times [\mathrm{I}_m^+(Q_n) \cos(m\chi) \cos(\varphi_0) - \mathrm{I}_m^-(Q_n) \sin(m\chi) \sin(\varphi_0)]$$

$$+ \mathrm{i}\sum_{n=1}^{\infty} c_n F_n (n+1/2)\, b_n \sum_{m=1}^{n} [-\mathrm{i}/(n+1/2)]^m\, m\pi_n^m(\theta)$$

$$\times [\mathrm{I}_m^-(Q_n) \cos(m\chi) \cos(\varphi_0) - \mathrm{I}_m^+(Q_n) \sin(m\chi) \sin(\varphi_0)] \ , \qquad (4b)$$

where

$$c_n \equiv (2n+1)/[n(n+1)] \qquad (5a)$$

$$F_n \equiv \exp(-\rho_0^2/w_0^2) \exp[-s^2 (n+1/2)^2] \qquad (5b)$$

$$Q_n \equiv (n+1/2)\, \varepsilon \qquad (5c)$$

$$\varepsilon \equiv 2s\rho_0/w_0 \qquad (5d)$$

$$\chi \equiv \varphi - \varphi_0 \ , \qquad (5e)$$

$$\mathrm{I}_m^{\pm}(Q_n) \equiv \mathrm{I}_{m-1}(Q_n) \pm \mathrm{I}_{m+1}(Q_n) \qquad (5f)$$

and $\mathrm{I}_m(Q_n)$ is a modified Bessel function. The scattering amplitudes for an incident localized model Gaussian beam that is *y*-polarized at the center of its focal waist is given by Eqs.(17a),(17b) of [1]. The scattering amplitude S_2 for a *y*-polarized beam is identical to S_1 for an *x*-polarized beam with a_n and b_n interchanged. Similarly, S_1 for a *y*-polarized beam is the negative of S_2 for an *x*-polarized beam with a_n and b_n interchanged. When the incident beam is polarized in the vertical *x* direction and the scattering plane is the horizontal *yz* plane with $\varphi=\pm 90°$, the VV scattering amplitude is $S_1(\theta,\varphi;\rho_0,\varphi_0)$ and the VH scattering amplitude is $S_2(\theta,\varphi;\rho_0,\varphi_0)$. When the incident beam is polarized in the horizontal *y* direction, the HV scattering amplitude is $S_1(\theta,\varphi;\rho_0,\varphi_0)$ and the HH scattering amplitude is $S_2(\theta,\varphi;\rho_0,\varphi_0)$.

3. Approximate Analytic Evaluation of the Sum over *m* for $0° \ll \theta \ll 180°$

The purpose of this Section is to develop a transitional approximation to the scattering amplitudes in the short wavelength limit $\lambda \ll a$ and for scattering angles away from 0° and 180° so that the sums over azimuthal modes *m* in Eqs.(4a),(4b) can be evaluated analytically. The sums over *m* contain modified Bessel functions $\mathrm{I}_m(Q_n)$, the GLMT angular functions $m\pi_n^m(\theta)$ and $\tau_n^m(\theta)$, sines and cosines of $m\chi$, and the factor $[-\mathrm{i}/(n+1/2)]^m$. The key to the analytical evaluation is a series expansion of the GLMT angular functions, which fortunately cancels the $1/(n+1/2)^m$ factor. This approximation is developed in a number of stages as follows.

3a. Approximation to the Amplitude of the Associated Legendre Functions

The angular functions $m\pi_n^m(\theta)$ and $\tau_n^m(\theta)$ of Eqs.(3a),(3b) are obtained from the associated Legendre functions $P_n^m[\cos(\theta)]$. For $n \gg 1$ and $0° \ll \theta \ll 180°$, the associated Legendre functions are rapidly oscillatory with a slowly varying θ-dependent amplitude. Their asymptotic expansion in this regime is given by Eq.(8.721.1) on p.962 of [4], (which corrects a misprint in Eq.(8.721.1) on p.1002 of the first edition, and whose overall sign has been adjusted to the convention used for associated Legendre polynomials in [3]),

$$P_n^m[\cos(\theta)] = (-1)^{-m} (2/\pi^{1/2}) \Gamma(n+m+1) \sum_{k=0}^{\infty} [\Gamma(m+k+1/2) / \Gamma(m-k+1/2)]$$

$$\times \cos[\Phi_k(\theta)] / \{k! \, \Gamma(n+k+3/2) \, [2 \sin(\theta)^{k+1/2}]\} \, , \qquad (6)$$

where $\Gamma(x)$ is the gamma function and

$$\Phi_k(\theta) = (n+k+1/2)\theta + (2k-1)\pi/4 + m\pi/2 \, . \qquad (7)$$

The dominant periodicity of $P_n^m[\cos(\theta)]$ is given by $\Phi_0(\theta)$. The $\Phi_k(\theta)$ terms for $k \geq 1$ describe progressively smaller distortions to the dominant periodicity. The divergence of the $[1/\sin(\theta)]^{k+1/2}$ factor as $\theta \rightarrow 0°$, 180° limits the region in which the series can be expected to be an accurate approximation of $P_n^m[\cos(\theta)]$ to $0° \ll \theta \ll 180°$. We will discuss how far from 0° and 180° this approximation can be expected to be accurate in Secs.4,5d here and in Sec. 3 of [2]. In Sec.5 of [2] we also discuss the effects of low partial waves for which Eq.(6) is not expected to be accurate.

The first thing that needs to be done is to obtain a judiciously chosen approximation to the magnitude of the dominant k=0 oscillation. This is helped by the fact that the value of $P_n^m[\cos(\theta)]$ is exactly known at θ=90°, and is given by Eq.(12.5.3) of [3]. Correcting a misprint in this equation, (see Eq.(8.6.1) of [5] which uses a different convention for $P_n^m[\cos(\theta)]$),

$$|P_n^m(0)| = (n+m)! \, / \, \{2^n \, [(n+m)/2]! \, [(n-m)/2]!\} \quad \text{for} \quad n+m=\text{even}$$

$$= 0 \quad \text{for} \quad n+m=\text{odd} \, . \qquad (8)$$

Our consideration of the magnitude of the associated Legendre functions allows us to temporarily set aside the sign of $P_n^m(0)$ and study the convergence rate of the k sum in Eq.(6). Expressing $\Gamma(n+3/2)$ in terms of factorials, the first four terms of Eq.(6) evaluated at θ=90° are

$$|P_n^m(0)| \approx (2/\pi)^{1/2} \, (n+m)! \, (n)! \, 2^{2n} \, / \, [(2n)! \, (n+1/2) \, \pi^{1/2}]$$

$$\times \{1 - (1/2) \, (m^2-1/4) \, / \, (n+3/2)$$

$$+ (1/8) \, (m^2-9/4) \, (m^2-1/4) \, / \, [(n+5/2) \, (n+3/2)]$$

$$- (1/48) \, (m^2-25/4) \, (m^2-9/4) \, (m^2-1/4)$$

$$/ \, [(n+7/2) \, (n+5/2) \, (n+3/2)]\} \, . \qquad (9)$$

The asymptotic series is expected to converge when $m^2/n < 1$ since each additional term in the series contains one additional factor of approximately this ratio. Consider for example the specific case of n=30, m=6. The exact value of $|P_{30}^6(0)|$ is 1.1297×10^8, whereas the first four terms of the asymptotic series give

$$|P_{30}^6(0)| \approx 2.0178 \times 10^8 \, (1.0000 - 0.5675 + 0.1473 - 0.0218)$$

$$= 1.1259 \times 10^8, \qquad (10)$$

which is only 0.34% lower than the exact value. The next term in the series is positive, and if it were included as well, the comparison would be even closer. As seen in Eq.(10), the k=0 term alone for n=30, m=6 and θ=90° is 2.0178×10^8, which is 78.6% higher than the exact value. The $k\geq1$ terms in the asymptotic series correct this k=0 overestimate back toward the exact value.

As an alternative to the above approach, van de Hulst used a very accurate one-term approximation to $P_n^0[\cos(\theta)]$ for $n\gg1$ and $0°\ll\theta\ll180°$ (see Eq.(5.4) of [6] where the approximation is attributed to p.117 of [7]). When the van de Hulst approximation is generalized to higher values of m as in Eq.(45) of [8] the result is not the first term of the asymptotic series, but is instead

$$|P_n^m(\theta)| \approx (n+1/2)^m \{2 / [\pi (n+1/2) \sin(\theta)] \}^{1/2} . \quad (11)$$

For the case of n=30, m=6 considered here, the van de Hulst approximation gives $|P_{30}^6(0)| \approx 1.1630\times10^8$, which is 2.95% higher than the exact value. This approximation is remarkably convenient for simplifying the sums over azimuthal modes m since the $(n+1/2)^m$ factor in Eq.(11) exactly cancels the $1/(n+1/2)^m$ factor in the scattering amplitudes of Eqs.(4a),(4b). Using this approximation for the m=±1 associated Legendre functions, van de Hulst obtained an approximation to the Lorenz-Mie scattering functions

$$\pi_n^1(\theta) \approx \Pi_n(\theta) \quad (12a)$$

$$\tau_n^1(\theta) \approx T_n(\theta) \ , \quad (12b)$$

where for the remainder of this study the functions $\Pi_n(\theta)$ and $T_n(\theta)$ are defined as (see p.212 of [9])

$$\Pi_n(\theta) \equiv [1/\sin(\theta)] \{2(n+1/2) / [\pi \sin(\theta)]\}^{1/2} \sin[(n+1/2)\theta - \pi/4] \quad (13a)$$

$$T_n(\theta) \equiv (n+1/2)\{2(n+1/2) / [\pi \sin(\theta)]\}^{1/2} \cos[(n+1/2)\theta - \pi/4] . \quad (13b)$$

If all one is interested in is the VV and HH scattering amplitudes, the one-term van de Hulst approximation to the GLMT angular functions would be sufficient to obtain close agreement with the exact GLMT co-polarized scattered intensities. But the VH and HV scattering amplitudes will be shown in Sec.4 to vanish at this level of approximation. They first appear only when the k=1 term of the asymptotic series of Eq.(6) is included as well. Thus the approximation to the GLMT angular functions required in this study requires more accuracy than the van de Hulst one-term approximation is capable of giving.

We therefore seek an approximation to the amplitude of the dominant k=0 periodicity of the associated Legendre functions that has a structure similar to that of Eq.(11), but that provides a close approximation to the first term of the asymptotic expansion of Eq.(6). The $k\geq1$ terms in the series will then correct this k=0 term back toward the exact result. On the basis of an analytical approximation to the factorials in Eq.(9), we found that the corrected amplitude

$$|P_n^m(0)| \approx (n+1/2)^m \{2 / [\pi (n+1/2)] \}^{1/2} \{1 + (1/2)[m^2/(n+1/2)]\} \quad (14)$$

serves our purposes well. For the case of n=30, m=6, the corrected magnitude is

$$|P_{30}^6(0)| \approx 1.1630\times10^8 \{1 + 0.5902\} = 1.8494\times10^8, \quad (15)$$

which is 8.35% lower than the 2.0178×10^8 magnitude of Eq.(10). If yet greater accuracy was required, another term proportional to $m^4/(n+1/2)^2$ could be added to the last factor in Eq.(14), the coefficient of which would have to be obtained by numerical experimentation. This additional term will be shown in Sec.4 to have only a minor influence, and will not be considered further here.

3*b. Approximation to the GLMT angular functions*

Using Eq.(14) to approximate the magnitude of the dominant k=0 oscillation in Eq.(6), the corrected approximation to the $0 \le k \le 3$ terms of the asymptotic expansion of the associated Legendre functions for $n \gg 1$ is

$$\begin{aligned} P_n^m[\cos(\theta)] \approx (-1)^m\,(n+1/2)^m\,\{2 / [\pi\,(n+1/2)\sin(\theta)]\}^{1/2} \\ \times\{1 + (1/2)[m^2/(n+1/2)]\}\{\cos[\Phi_0(\theta)] \\ + [(1/2)\,(m^2-1/4)/(n+3/2)]\cos[\Phi_1(\theta)] / \sin(\theta) \\ + [(1/8)\,(m^2-9/4)\,(m^2-1/4)/(n+5/2)\,(n+3/2)]\cos[\Phi_2(\theta)] / \sin^2(\theta) \\ + [(1/48)\,(m^2-25/4)\,(m^2-9/4)\,(m^2-1/4) \\ / (n+7/2)\,(n+5/2)\,(n+3/2)]\cos[\Phi_3(\theta)] / \sin^3(\theta)\} \ , \end{aligned} \tag{16}$$

where the dominant periodicity is

$$\Phi_0(\theta) = (n+1/2)\theta + m\pi/2 - \pi/4 \ , \tag{17a}$$

and the progressively smaller distortions to it are

$$\Phi_1(\theta) = \Phi_0(\theta) + \theta + \pi/2 \tag{17b}$$

$$\Phi_2(\theta) = \Phi_0(\theta) + 2\theta + \pi \tag{17c}$$

$$\Phi_3(\theta) = \Phi_0(\theta) + 3\theta + 3\pi/2 \ . \tag{17d}$$

Substituting the k=0,1 terms of the asymptotic expansion for $P_n^m[\cos(\theta)]$ into Eqs.(3a),(3b), the first few terms of the corresponding asymptotic expansion of the GLMT angular functions are

$$m\pi_n^m(\theta) \approx K_m\,(C_1\,m + C_3\,m^3) \quad \text{for even } m \tag{18a}$$

$$\approx \mathrm{i}\,K_m\,(D_1\,m + D_3\,m^3) \quad \text{for odd } m \ , \tag{18b}$$

where

$$K_m \equiv (-\mathrm{i})^m\,(n+1/2)^{m-1} \tag{19}$$

$$N_n(\theta) \equiv (n+1/2)\sin(\theta) \tag{20}$$

and

$$C_1 = T_n(\theta)/N_n(\theta) \tag{21a}$$

$$D_1 = \Pi_n(\theta) \tag{21b}$$

$$C_3 = -\,(1/2)\cos(\theta)\,\Pi_n(\theta)/N_n(\theta) \tag{22a}$$

$$D_3 = (1/2)\cos(\theta)\,T_n(\theta)/N_n^2(\theta) \ . \tag{22b}$$

Similarly,

$$\tau_n^m(\theta) \approx K_m\,(A_0 + A_2\,m^2) \quad \text{for even } m \tag{23a}$$

$$\approx i\, K_m\, (B_0 + B_2\, m^2) \quad \text{for odd } m\,, \tag{23b}$$

where

$$A_0 = -\, \Pi_n(\theta)\, N_n(\theta)$$
$$-\, (3/8)\cos(\theta)\, T_n(\theta)/N_n(\theta)$$
$$-\, (1/8)\sin(\theta)\, \Pi_n(\theta) \tag{24a}$$

$$B_0 = T_n(\theta)$$
$$-\, (3/8)\cos(\theta)\, \Pi_n(\theta)$$
$$+\, (1/8)\sin(\theta)\, T_n(\theta)/N_n(\theta) \tag{24b}$$

$$A_2 = -\, (1/2)\cos(\theta)\, T_n(\theta)/N_n(\theta)$$
$$-\, (1/16)\sin(\theta)\cos(\theta)\, T_n(\theta)/N_n^2(\theta)$$
$$+\, (7/16)\cos^2(\theta)\, \Pi_n(\theta)/N_n(\theta)$$
$$+\, (1/4)\sin^2(\theta)\, \Pi_n(\theta)/N_n(\theta) \tag{25a}$$

$$B_2 = -\, (1/2)\cos(\theta)\, \Pi_n(\theta)$$
$$-\, (1/16)\sin(\theta)\cos(\theta)\, \Pi_n(\theta)/N_n(\theta)$$
$$-\, (7/16)\cos^2(\theta)\, T_n(\theta)/N_n^2(\theta)$$
$$-\, (1/4)\sin^2(\theta)\, T_n(\theta)/N_n^2(\theta)\,. \tag{25b}$$

These expressions require a number of comments. For $n \gg 1$, the factor of $(n+1/2)^{m-1}$ in K_m of Eq.(19) means that the magnitude of the GLMT angular functions rapidly becomes quite large as m increases. This was seen in the case of n=30, m=6 treated above. This rapid increase in value produces some uncertainty as to the best place to cut off the m sums in numerical computations. But the $1/(n+1/2)^m$ factor in Eqs.(4a),(4b) cancels away the rapid increase in the GLMT angular functions. The point of view taken here is that by allowing this cancellation occur analytically rather than numerically where it is more difficult to identify and interpret, one will hopefully obtain a useful simplification of the equations. The various terms of the series expansion of the GLMT angular functions have a number of significant properties. (i) The terms in the series for $m\pi_n^m(\theta)$ are proportional to odd powers of m, and the terms in the series for $\tau_n^m(\theta)$ are proportional to even powers of m. If $k \geq 2$ terms in the asymptotic expansion of $P_n^m[\cos(\theta)]$ had been included, higher powers of m would have occurred in Eqs.(18),(23). (ii) The function $\Pi_n(\theta)$ of Eq.(13a) is a factor of $(n+1/2)$ smaller in magnitude than $T_n(\theta)$ of Eq.(13b), and so one can assume that $\Pi_n(\theta) \ll T_n(\theta)$ when $n \gg 1$ and θ is not near one of the zeros of $T_n(\theta)$. (iii) Equations (21),(22),(24),(25) for $m\pi_n^m(\theta)$ and $\tau_n^m(\theta)$ contain $\Pi_n(\theta)$ and $T_n(\theta)/N_n(\theta)$ as a pair conjugate functions of roughly equal magnitude for even and odd m. (iv) Equations (18)-(25) give the first few terms in a series expansion of the GLMT angular functions in powers of $(1/n)$ and (m^2/n). We are assuming here that $n \gg 1$ and $(m^2/n) < 1$. As a shorthand, let $T_n(\theta)$ be of order (T). Then $\Pi_n(\theta)$ is of order (T/n). Using the k=0,1 terms of the asymptotic series of the associated Legendre functions of Eq.(6), C_1 and D_1 are of order (mT/n) and give the dominant contribution to $m\pi_n^m(\theta)$. The terms C_3 and D_3 are of order (m^3T/n^2) and are corrections to the dominant contribution. Smaller corrections of order (mT/n^2), (m^3T/n^3), and (m^5T/n^3) also result from the k=1 term of the asymptotic series, but have been omitted in Eqs.(18)-(22). One should note that the rate of convergence of terms with higher powers of (m^2/n) is expected to be significantly slower than those with

higher powers of $(1/n)$. No terms of order (mT/n) or (m^3T/n^2), in addition to those given in Eqs.(21),(22), occur if either the k=2 term of the asymptotic series or the postulated third term of the k=0 amplitude correction mentioned following Eq.(15) are considered.

Similarly, using the k=0,1 terms of the asymptotic series of the associated Legendre functions, the first term in A_0 and B_0 of Eqs.(24a),(24b) is of order (T) and is the dominant contribution to $\tau_n^m(\theta)$. The first term of A_2 and B_2 is of order (m^2T/n) and is a correction to the dominant contribution. The last two terms of A_0 and B_0 are of order (T/n) and are smaller corrections, and the final three terms of A_2 and B_2 are of order (m^2T/n^2) and are yet smaller corrections. The k=1 term of the asymptotic series also gives rise to smaller corrections of order (T/n^2), (m^2T/n^3), (m^4T/n^2), and (m^4T/n^3) which have been omitted. No additional terms of order (T), (T/n), (m^2T/n), and (m^2T/n^2), in addition to those given in Eqs.(24),(25), occur if either the k=2 term of the asymptotic series or the postulated third term of the k=0 amplitude correction are considered. Thus the series expansions of A_0, B_0, C_1, D_1, A_2, B_2, C_3, D_3 in powers of $1/(n+1/2)$ should be rapidly convergent for $n\gg1$, hopefully requiring only a small number of such terms for an accurate evaluation of S_1 and S_2.

3c. Analytical Evaluation of the m Sums

The series expansions of the GLMT angular functions of Eqs.(18)-(25) are now inserted into the sums over m in S_1 and S_2 of Eqs.(4a),(4b). The sums now have the form

$$\sum_{m=0}^{n}{}^{(\text{e or o})}\, m^p\, I_m(Q_n)\, \{\cos(m\chi) \text{ or } \sin(m\chi)\}\,, \tag{26}$$

where p is an integer power, I_m is a modified Bessel function, Q_n and χ are given by Eqs.(5c),(5e), and the sum is over either even (e) or odd (o) non-negative values of m. Since for large Q_n, the modified Bessel functions I_m become nearly exponential in Q_n and independent of m, (see Eq.(11.136) of [3]) performing the m sums analytically should result in further simplifications of S_1 and S_2. All the required sums can be exactly evaluated analytically using the generating functions for modified Bessel functions if the upper limit of the sum is changed from $n\gg1$ to infinity (see Eqs.(9.1.44),(9.1.45) of [5] and Eq.(11.110) of [3]). For p=0, one obtains

$$\sum_{m=1}^{\infty}{}^{(\text{o})}\, \mathrm{I}_m^{+}(Q_n)\, \cos(m\chi) = \cosh[Q_n \cos(\chi)]\, \cos(\chi) \tag{27a}$$

$$\mathrm{I}_1(Q_n) + \sum_{m=2}^{\infty}{}^{(\text{e})}\, \mathrm{I}_m^{+}(Q_n)\, \cos(m\chi) = \sinh[Q_n \cos(\chi)]\, \cos(\chi) \tag{27b}$$

$$\sum_{m=1}^{\infty}{}^{(\text{o})}\, \mathrm{I}_m^{-}(Q_n)\, \sin(m\chi) = \cosh[Q_n \cos(\chi)]\, \sin(\chi) \tag{27c}$$

$$\sum_{m=2}^{\infty}{}^{(\text{e})}\, \mathrm{I}_m^{-}(Q_n)\, \sin(m\chi) = \sinh[Q_n \cos(\chi)]\, \sin(\chi)\ . \tag{27d}$$

The sums for $p\geq1$ are evaluated by repeated differentiation of Eqs.(27a)-(27d) with respect to χ. However, progressively higher order derivatives will produce higher powers of the multiplicative factor Q_n. Since Q_n is proportional to ε of Eq.(5d), as long as $\varepsilon\ll1$ these higher order terms will make progressively smaller contributions to the scattering amplitudes S_1 and S_2. Lastly, it should be noted that the sums over m given above, but with I_m^{+} replaced by I_m^{-} and I_m^{-} replaced by I_m^{+}, cannot be evaluated using the generating function for modified Bessel functions. Thus it appears most fortuitous that the sums appearing in the approximation to S_1 and S_2 are those which can be analytically evaluated.

When the sums over m in the scattering amplitudes are exactly analytically evaluated with the upper limit of the sum increased to infinity, the various order contributions to the scattering amplitudes are organized differently than they were for the GLMT angular functions. For example, corrections to the GLMT angular functions of order (T/n^2) and (m^2T/n^2) arising from the k=2 term of the asymptotic expansion of the associated Legendre functions of Eq.(6) were calculated in Sec.3b. But corrections to the angular functions of order (m^4T/n^2) resulting from the postulated third term of the approximation of the dominant k=0 amplitude described following Eq.(15) were not. When the sums over m are evaluated analytically for each of these three corrections to the angular functions, they all produce corrections to the scattering amplitudes of order (T/n^2). Since all such corrections of order (m^pT/n^2) were not calculated here, they will not be considered further. Thus in Sec.3d, only the terms in the scattering amplitudes of order (T) and (T/n) are included. Specifically, A_2 and B_2 of Eqs.(25a),(25b) are truncated at

$$A_2 = - (1/2) \cos(\theta)\, T_n(\theta)/N_n(\theta) \tag{28a}$$

$$B_2 = - (1/2) \cos(\theta)\, \Pi_n(\theta) \tag{28b}$$

and Eqs.(22a),(22b) are replaced by

$$C_3 = 0 \tag{28c}$$

$$D_3 = 0 \, . \tag{28d}$$

3d. Approximation of the Scattering Amplitudes

Substituting the sums over m for $0 \le p \le 3$ into Eqs.(4a),(4b), one obtains expressions for the off-axis scattering amplitudes $S_1(\theta,\varphi;\rho_0,\varphi_0)$ and $S_2(\theta,\varphi;\rho_0,\varphi_0)$ for the arbitrary off-axis beam position (ρ_0, φ_0) and scattering plane orientation φ, in which the only sum to be evaluated numerically is the sum over partial waves n. For an incident x-polarized off-axis localized model Gaussian beam one obtains

$$\begin{aligned} S_1(\theta,\varphi;\rho_0,\varphi_0) \approx \sum_{n=1}^{\infty} c_n F_n b_n \{ & (ch) \sin(\varphi) R_1(\theta) + \mathrm{i}\, (sh) \sin(\varphi) R_2(\theta) \\ & + \mathrm{i}\, (ch) \cos(\varphi) R_3(\theta) + (sh) \cos(\varphi) R_4(\theta) \} \\ + \sum_{n=1}^{\infty} c_n F_n a_n \{ & (ch) \sin(\varphi) R_5(\theta) + \mathrm{i}\, (sh) \sin(\varphi) R_6(\theta) \\ & + \mathrm{i}\, (ch) \cos(\varphi) R_7(\theta) + (sh) \cos(\varphi) R_8(\theta) \} \, , \end{aligned} \tag{29}$$

where (ch) and (sh) are shorthand symbols for

$$(ch) \equiv \cosh[Q_n \cos(\chi)] \tag{30a}$$

$$(sh) \equiv \sinh[Q_n \cos(\chi)] \, , \tag{30b}$$

and

$$R_1(\theta) = B_0 + B_2 [1 - Q_n^2 \sin^2(\chi)] + \mathrm{i}\, A_2 Q_n \cos(\chi) \tag{31a}$$

$$R_2(\theta) = A_0 + A_2 [1 - Q_n^2 \sin^2(\chi)] - \mathrm{i}\, B_2 Q_n \cos(\chi) \tag{31b}$$

$$R_3(\theta) = 2A_2 Q_n \sin(\chi) \tag{31c}$$

$$R_4(\theta) = 2B_2\, Q_n \sin(\chi) \tag{31d}$$

$$R_5(\theta) = D_1 \tag{31e}$$

$$R_6(\theta) = C_1 \tag{31f}$$

$$R_7(\theta) = C_1\, Q_n \sin(\chi) \tag{31g}$$

$$R_8(\theta) = D_1\, Q_n \sin(\chi)\ . \tag{31h}$$

Similarly,

$$\begin{aligned} S_2(\theta,\varphi;\rho_0,\varphi_0) \approx \sum_{n=1}^{\infty} c_n F_n a_n \{&(ch)\cos(\varphi)\, R_1(\theta) + \mathrm{i}\,(sh)\cos(\varphi)\, R_2(\theta) \\ &- \mathrm{i}\,(ch)\sin(\varphi)\, R_3(\theta) - (sh)\sin(\varphi)\, R_4(\theta)\} \\ + \sum_{n=1}^{\infty} c_n F_n b_n \{&(ch)\cos(\varphi)\, R_5(\theta) + \mathrm{i}\,(sh)\cos(\varphi)\, R_6(\theta) \\ &- \mathrm{i}\,(ch)\sin(\varphi)\, R_7(\theta) - (sh)\sin(\varphi)\, R_8(\theta)\}\ . \end{aligned} \tag{32}$$

As was the case for the exact GLMT scattering amplitudes, the approximation to the scattering amplitudes for an incident *y*-polarized off-axis localized model Gaussian beam is given by the following prescription. The approximate scattering amplitude S_2 for a *y*-polarized beam is identical to S_1 for an *x*-polarized beam with a_n and b_n interchanged, and S_1 for a *y*-polarized beam is the negative of S_2 for an *x*-polarized beam with a_n and b_n interchanged. The region of validity of Eqs.(29)-(32) is nominally $0° \ll \theta \ll 180°$, where the exact interval is expected to depend on the specific beam and particle parameters chosen. This point will be discussed further in Secs.4,5d below and in Sec.3 of [2]. In addition, the validity of the series expansion of the GLMT angular functions assumed that $n \gg 1$. In Lorenz-Mie theory this corresponds to scattering in the short wavelength limit, $\lambda \ll a$, where the contribution of large partial waves is more important than that of small partial waves (see Sec.12.33 of [9]).

4. Simplifications for Co-Polarized and Crossed-Polarized Scattering

We now limit our interest to the scattering geometry described in Sec.1 with the scattering plane horizontal, φ=90°. In the first case examined here, the incident Gaussian beam is translated off-axis in the scattering plane with φ_0=-90°. Substituting into Eqs.(31a)-(31h), the co-polarized scattering amplitudes are given by the $R_i(\theta)$ terms with i=1, 2, 5, 6,

$$\begin{aligned} S_{VV}(\theta;\rho_0) \approx \sum_{n=1}^{\infty} c_n F_n b_n \{&\cosh(Q_n)\,[B_0 + B_2\,(1 - Q_n^{\,2}) - \mathrm{i}\, A_2\, Q_n] \\ &- \mathrm{i}\sinh(Q_n)\,[A_0 + A_2\,(1 - Q_n^{\,2}) + \mathrm{i}\, B_2\, Q_n]\} \\ + \sum_{n=1}^{\infty} c_n F_n a_n\, &[\cosh(Q_n)\, D_1 - \mathrm{i}\sinh(Q_n)\, C_1] \end{aligned} \tag{33a}$$

and

$$S_{HH}(\theta;\rho_0) \approx \sum_{n=1}^{\infty} c_n F_n a_n \{\cosh(Q_n) [B_0 + B_2 (1 - Q_n^2) - i A_2 Q_n]$$

$$- i \sinh(Q_n) [A_0 + A_2 (1 - Q_n^2) + i B_2 Q_n]\}$$

$$+ \sum_{n=1}^{\infty} c_n F_n b_n [\cosh(Q_n) D_1 - i \sinh(Q_n) C_1] \quad . \qquad (33b)$$

The cross-polarized scattering amplitudes are

$$S_{VH}(\theta;\rho_0) = S_{HV}(\theta;\rho_0) = 0 \quad . \qquad (34)$$

The scattering amplitudes $S_{VV}(\theta)$ and $S_{HH}(\theta)$ were computed for the beam parameters $\lambda = 0.5145$ μm, $\rho_0 = 40$μm, $\varphi_0 = -90°$, $w_0 = 20$μm and the particle parameters $a = 43.3$ μm, M=1.33 of [8] in the φ=90° scattering plane for $0° \le \theta \le 360°$. The red curves in Figs.1,2 are the exact localized model GLMT scattered VV and HH intensity, respectively, and the blue curves are the approximation of Eqs.(33a),(33b), consisting of the dominant term of order (T) and the first order correction of order (T/n). Since the approximation diverges as $\theta \to 0°, 180°$ (see for example Fig.3 of [2]), it is shown in Figs.1-6 for $1.9° \le \theta \le 178.1°$. In addition, although the approximation was expected in Sec.3a to be valid for $n \gg 1$, the numerical computations leading to Figs.1-6 used it for all partial waves. Examination of Figs.1,2 shows that the magnitude of the approximation for both co-polarization states is in good agreement with that of the exact GLMT intensity over many decades for virtually the entire scattering angle interval. The greatest difference between the exact GLMT and approximate intensity occurs when the intensity is the weakest, due to the delicate destructive interference of the partial wave contributions. The phase of the high spatial frequency oscillations in the approximate intensity is seen to drift with respect to that of the oscillations in the exact GLMT intensity in a number of places, and certainly could affect the extent of destructive interference in the regions of weakest intensity mentioned above. The VV intensity oscillations in Fig.1 are in-phase in the first- and second-order rainbow regions and at θ~90°, they appear to be about 90° out of phase at θ~70°, 340°, and they are 180° out of phase at θ~20°, 290°, and for the external reflection ripple superimposed on the principal peak of the second-order rainbow. The situation in Fig.2 for the HH intensity is similar. If a detector array is sufficiently coarse so as to average over the high spatial frequency intensity oscillations, the angle-averaged intensity of the approximation matches that of the exact GLMT intensity quite well. But the phase drift of the oscillations in the approximation can have significant consequences, as will be seen in [2] where time-domain scattering is considered.

As a further approximation to S_{VV} and S_{HH} for an off-axis beam in the scattering plane, the dominant portion of S_{VV} and S_{HH} of Eqs.(33a),(33b) of order (T) is,

$$S_{VV}(\theta;\rho_0) \approx \sum_{n=1}^{\infty} c_n F_n b_n [T_n(\theta) \cosh(Q_n) + i \Pi_n(\theta) N_n(\theta) \sinh(Q_n)] \quad . \qquad (35a)$$

and

$$S_{HH}(\theta;\rho_0) \approx \sum_{n=1}^{\infty} c_n F_n a_n [T_n(\theta) \cosh(Q_n) + i \Pi_n(\theta) N_n(\theta) \sinh(Q_n)] \quad . \qquad (35b)$$

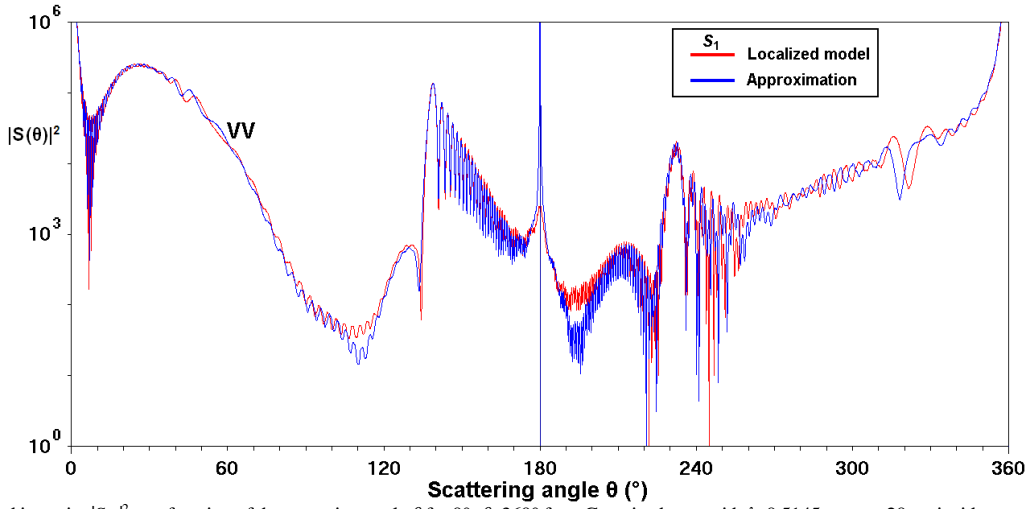

Fig.1: Scattered intensity $|S_{VV}|^2$ as a function of the scattering angle θ for $0°\leq\theta\leq360°$ for a Gaussian beam with λ=0.5145μm, w_0=20μm incident on a homogeneous spherical particle with a=43.3μm, M=1.33. The scattering plane is φ=90°, and the beam is off-axis in the scattering plane with ρ_0=40μm, φ_0=-90°. The scattered intensity $|S_{VH}|^2$ is identically zero. The exact GLMT result is given by the red curves, and the approximation of Secs.3,4 is given by the blue curves.

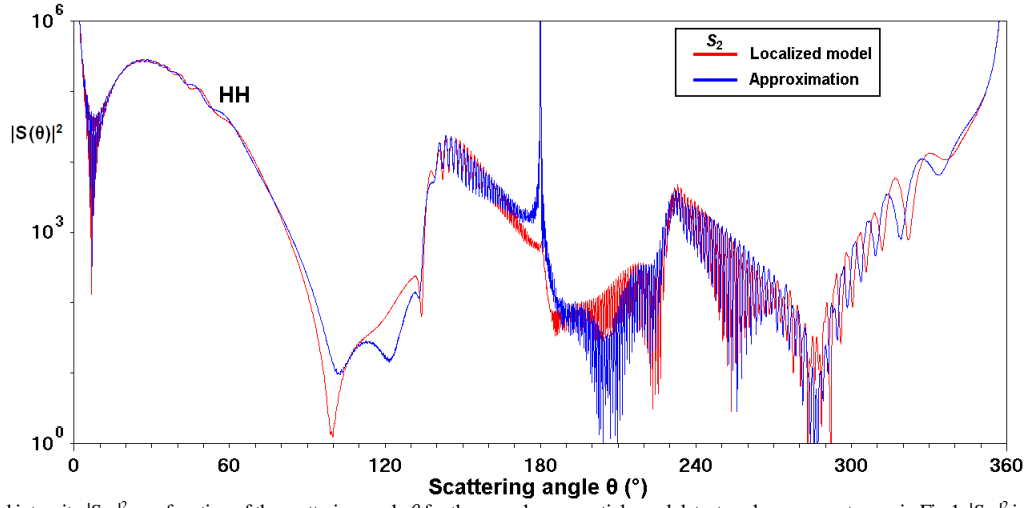

Fig.2: Scattered intensity $|S_{HH}|^2$ as a function of the scattering angle θ for the same beam, particle, and detector plane parameters as in Fig.1. $|S_{HV}|^2$ is identically zero. The exact GLMT result is given by the red curves, and the approximation of Secs.3,4 is given by the blue curves.

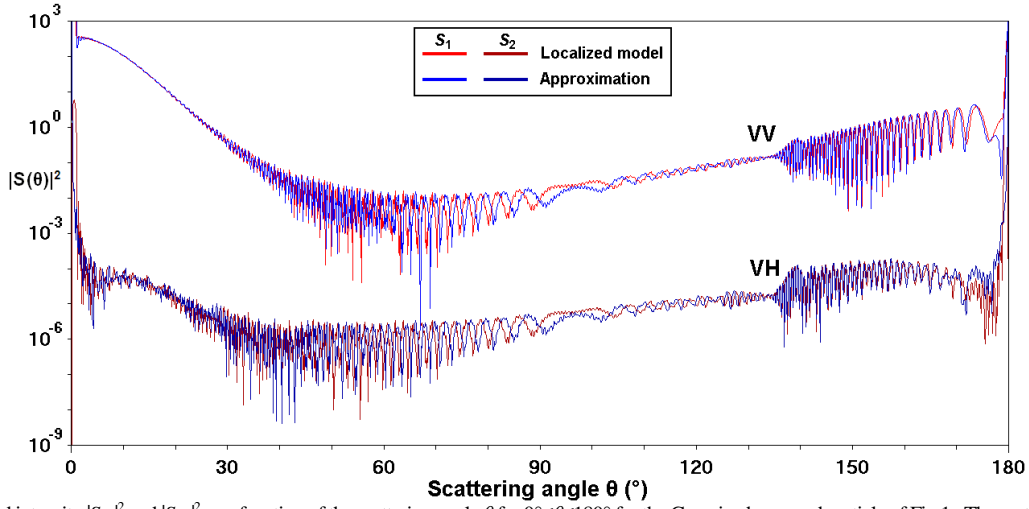

Fig.3: Scattered intensity $|S_{VV}|^2$ and $|S_{VH}|^2$ as a function of the scattering angle θ for $0°\leq\theta\leq180°$ for the Gaussian beam and particle of Fig.1. The scattering plane is φ=90°, and the beam is off-axis perpendicular to the scattering plane with off-axis incidence ρ_0=40μm, φ_0=180°. The exact GLMT result is given by the red curves, and the approximation of Secs.3,4 is given by the blue curves.

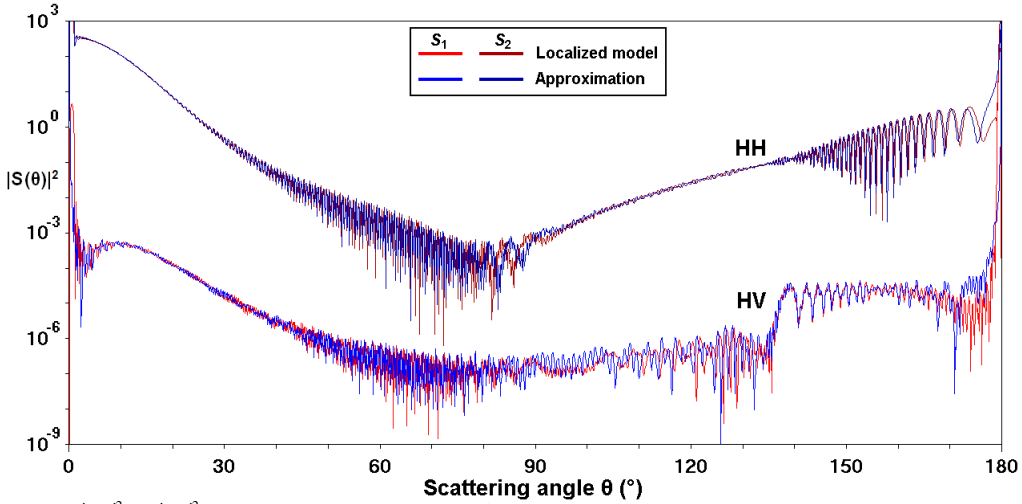

Fig.4: Scattered intensity $|S_{HH}|^2$ and $|S_{HV}|^2$ as a function of the scattering angle θ for the same beam, particle, and detector plane parameters as in Fig.3. The exact GLMT result is given by the red curves, and the approximation of Secs.3,4 is given by the blue curves.

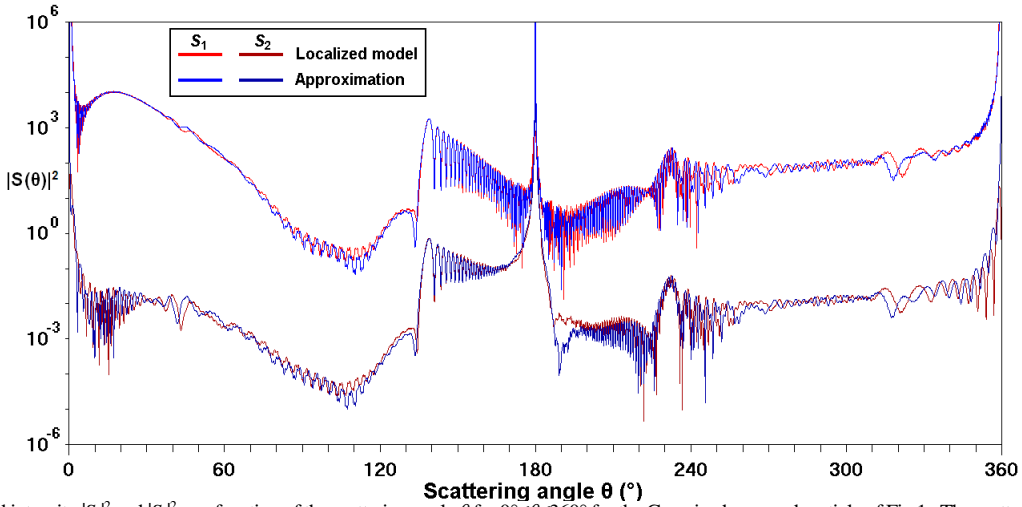

Fig.5: Scattered intensity $|S_1|^2$ and $|S_2|^2$ as a function of the scattering angle θ for $0°\leq\theta\leq360°$ for the Gaussian beam and particle of Fig.1. The scattering plane is φ=90°, and the beam is off-axis with ρ_0=40μm, φ_0=-45°. The exact GLMT result is given by the red curves, and the approximation of Secs.3,4 is given by the blue curves.

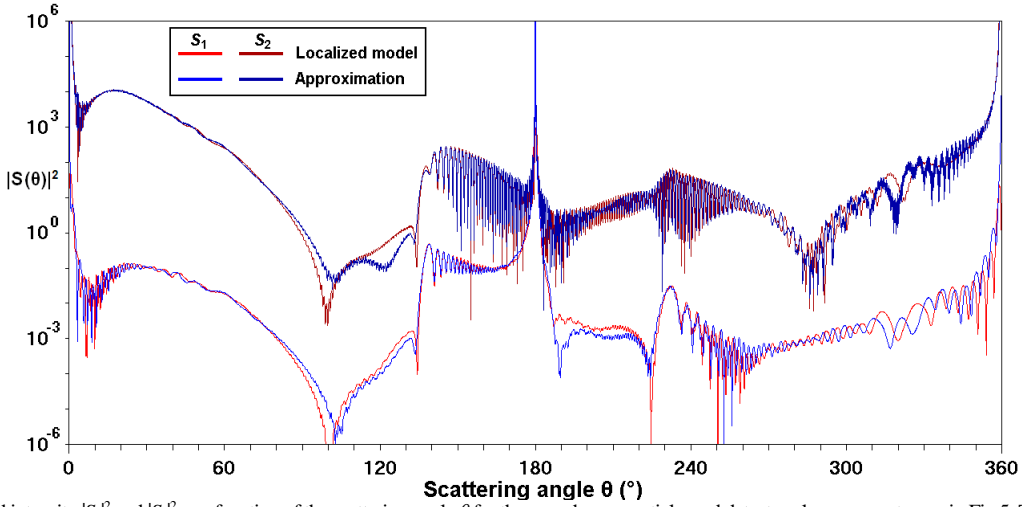

Fig.6: Scattered intensity $|S_1|^2$ and $|S_2|^2$ as a function of the scattering angle θ for the same beam, particle, and detector plane parameters as in Fig.5. The scattering plane is φ=90°, and the beam is off-axis with ρ_0=40μm, φ_0=45°. The exact GLMT result is given by the red curves, and the approximation of Secs.3,4 is given by the blue curves.

Numerical computations with Eqs.(35a),(35b) gave results that were virtually identical to the results of Figs.1,2 that used Eqs.(33a),(33b). In addition, $\cosh(Q_n)$ and $\sinh(Q_n)$ asymptotically approach (1/2) $\exp(Q_n)$ for $Q_n \gg 1$. For the example discussed here, the largest partial wave computed [10] is n_{max}=563 giving Q_{nmax}=9.0, which easily satisfies the $Q_n \gg 1$ condition. Substituting this further approximation into Eqs.(35a),(35b) one obtains

$$S_{VV}(\theta;\rho_0) \approx \sum_{n=1}^{\infty} c_n F_n \exp[(n+1/2)\,\varepsilon]\; b_n\,[T_n(\theta) + \mathrm{i}\,\Pi_n(\theta)\,N_n(\theta)]/2 \qquad (36a)$$

$$S_{HH}(\theta;\rho_0) \approx \sum_{n=1}^{\infty} c_n F_n \exp[(n+1/2)\,\varepsilon]\; a_n\,[T_n(\theta) + \mathrm{i}\,\Pi_n(\theta)\,N_n(\theta)]/2 \quad . \qquad (36b)$$

Equations (36a),(36b) are identical to the simple ray-theory-based approximation of Eqs.(43a),(43b),(47) of [1] with the $\cos[(n+1/2)\theta-\pi/4]$ term in $T_n(\theta)$ of Eqs.(12b),(13b) now replaced in Eqs.(36a),(36b) by (1/2) $\exp\{\mathrm{i}[(n+1/2)\theta-\pi/4]\}$, and agreeing with the convention used in Sec.5 of [11].

We next consider the case when the focused Gaussian beam is translated off-axis perpendicular to the scattering plane with φ_0=180°. For co-polarized scattering, substitution into Eqs.(31a)-(31h) gives the $R_i(\theta)$ terms with i=1, 5,

$$S_{VV}(\theta;\rho_0) \approx \sum_{n=1}^{\infty} c_n F_n \{b_n\,[B_0 + B_2\,(1 - Q_n^{\,2})] + a_n D_1\} \quad , \qquad (37a)$$

$$S_{HH}(\theta;\rho_0) \approx \sum_{n=1}^{\infty} c_n F_n \{a_n\,[B_0 + B_2\,(1 - Q_n^{\,2})] + b_n D_1\} \quad . \qquad (37b)$$

For future reference, the dominant order (T) term of S_{VV} and S_{HH} of Eqs.(37a),(37b) is

$$S_{VV}(\theta;\rho_0) \approx \sum_{n=1}^{\infty} c_n F_n b_n T_n(\theta) \quad , \qquad (38a)$$

$$S_{HH}(\theta;\rho_0) \approx \sum_{n=1}^{\infty} c_n F_n a_n T_n(\theta) \quad . \qquad (38b)$$

The amplitudes for crossed-polarized scattering include $R_i(\theta)$ terms with i=3,7,

$$S_{VH}(\theta;\rho_0) \approx \mathrm{i} \sum_{n=1}^{\infty} c_n F_n Q_n\,(2a_n A_2 + b_n C_1)$$

$$= -\mathrm{i} \sum_{n=1}^{\infty} c_n F_n Q_n\,[a_n \cos(\theta) - b_n]\; T_n(\theta)/N_n(\theta) \quad , \qquad (39a)$$

and

$$S_{HV}(\theta;\rho_0) \approx -\mathrm{i} \sum_{n=1}^{\infty} c_n F_n Q_n\,(2b_n A_2 + a_n C_1)$$

$$= - \mathrm{i} \sum_{n=1}^{\infty} c_n F_n Q_n [a_n - b_n \cos(\theta)] T_n(\theta)/N_n(\theta) \quad . \qquad (39b)$$

Equations (37)-(39) require a number of comments. (i) It is sensible that the cross-polarized scattering amplitudes $S_{VH}(\theta)$ and $S_{HV}(\theta)$ contain roughly similar amounts of TE (i.e. b_n) and TM (i.e. a_n) contributions. (ii) The dominant term of S_{VH} and S_{HV} of Eqs.(39a),(39b) is of the same order, (T/n), as the first correction to the dominant term of S_{VV} and S_{HH} in Eqs.(37a),(37b). The first order correction to the cross-polarized scattering amplitudes, of order (T/n^2), was not included for the reasons mentioned in the discussion following Eqs.(27a)-(27d). This could be potentially problematical since our final expressions for $\tau_n^m(\theta)$ and $m\pi_n^m(\theta)$ are the result of a number of approximations that are valid for only large partial waves, $n \gg 1$, and small azimuthal modes, $m^2/(n+1/2)<1$. This makes the VH and HV intensities of Eqs.(39a),(39b) potentially more sensitive to the accuracy of all the approximations than are the VV and HH intensities of Eqs.(37a),(37b) . (iii) This concern turns out to be unwarranted. Figures 3,4 show the VV, VH and the HV, HH scattered intensities, respectively for the incident beam translated off-axis perpendicular to the scattering plane with ρ_0=40μm and φ_0=180°. The red curves are the exact GLMT polarization-resolved intensities and the blue curves are the approximation of Eqs.(37),(39). Again, the magnitude of the approximation is in good agreement with the magnitude of the exact GLMT intensity for all four polarization channels over almost the entire angular interval $0° \le \theta \le 180°$. But the phase of the high spatial frequency oscillations in the approximation drifts with respect to the phase of the oscillations in the exact GLMT intensity. (iv) As was the case for φ_0=-90° mentioned above, the agreement with the VV and HH intensities is almost identical if only the dominant term of order (T) of Eqs.(38a),(38b) is used in the approximation instead of Eqs.(37a),(37b). (v) Equations (38a),(38b) for $S_{VV}(\theta)$ and $S_{HH}(\theta)$ are identical to the simple ray-theory-based approximation of Eqs.(43a),(43b),(48) of [1]. For the input parameters of Figs.1-4, one has w_0/a=0.46, and the CPU run time of the approximate scattered intensity as a function of θ was found to be almost exactly 1/7 of that for the exact GLMT equations. When w_0/a was decreased to 0.20 and 0.10, the CPU run time of the approximation fell to about 1/14 and 1/60, respectively, of that for the exact GLMT equations, indicating that the approximation is most numerically efficient for large particle sizes and narrowly focused beams.

Figures 5, 6 show the GLMT scattered intensities (the red and brown curves), and our approximation to them using Eqs.(29)-(32) (the blue curves), for the same beam and particle parameters as in Figs.1-4. The dominant $|S_1|^2$=VV intensity and the weaker $|S_2|^2$=VH intensity are shown in Fig.5 for φ=90°, φ_0=-45°, and the dominant $|S_2|^2$=HH intensity and the weaker $|S_1|^2$=HV intensity are shown in Fig.6 for φ=90°, φ_0=45°. The dominant intensities consist of the $R_i(\theta)$ terms of Eqs.(31a)-(31h) with i=1, 2, 5, 6, and the weaker intensities consist of i=3, 4, 7, 8. The $|S_1|^2$ intensity in Fig.5 is a much closer match to the VV intensity in Fig.1 than it is to the VV intensity in Fig.3. We believe this is due to the fact that the beam is located relatively near the incident Descartes ray position of the first- and second-order rainbows on the $-y$ axis. The weaker $|S_2|^2$ intensity in Fig.5, contrary to the VH intensity in Fig.3, clearly exhibits the first-order and second-order TE rainbows, and appears quite similar to the dominant $|S_1|^2$ intensity, except for being a number of orders of magnitude smaller. The $|S_2|^2$ intensity in Fig.6 is a much closer match to the HH intensity in Fig.2 than it is to the HH intensity in Fig.4. The weaker $|S_1|^2$ intensity also exhibits the first- and second-order TE rainbows. The reason for this will be discussed below. These results are similar to those that have recently appeared in Figs.7,8 of [12] for an incident elliptical Gaussian beam.

The cross-polarized scattering amplitudes may be further simplified for an arbitrary off-axis location of the Gaussian beam by substituting φ=90° for the horizontal scattering plane and Eq.(5c) for Q_n into Eqs.(29),(32), extracting the order (T/n) term of S_{VH} and S_{HV}, and then comparing the result to the order (T) term of S_{VV} and S_{HH}. In this approximation, one obtains

$$S_{VH}(\theta;\rho_0,\varphi_0) \approx -\mathrm{i}\varepsilon \cos(\varphi_0) [S_{VV}(\theta) - S_{HH}(\theta) \cos(\theta)] / \sin(\theta) \qquad (40a)$$

$$S_{HV}(\theta;\rho_0,\varphi_0) \approx -\mathrm{i}\varepsilon \cos(\varphi_0) [S_{VV}(\theta) \cos(\theta) - S_{HH}(\theta)] / \sin(\theta) \quad . \qquad (40b)$$

The factor of ε in Eqs.(40a),(40b) exactly matches the size of the amplitudes predicted on the basis of the circular symmetry breaking and the constraints imposed by Maxwell's equations in Secs.4d, 4e of [1]. At θ=90° the amplitude S_{VH} is purely TE-polarized and S_{HV} is purely TM-polarized. In addition, S_{VH} and S_{HV} are proportional to S_{VV}-S_{HH} for $\theta\approx$0° and are proportional to S_{VV}+S_{HH} for $\theta\approx$180°. Higher-order corrections to S_{VV} and S_{HH} will lead to terms in the expressions for S_{VH} and S_{HV} having higher powers of ε. The relationship between the co-polarized and cross-polarized scattering amplitudes of Eqs.(40a),(40b) explains why the numerical convergence for the exact GLMT scattering amplitudes S_{VV} and S_{HH} was achieved in [13] with m_{max}=10 for the sum over azimuthal modes m, while m_{max}=20 was required for convergence of S_{VH} and S_{HV}. Since S_{VV} and S_{HH} almost totally destructively interfere with each other for $\theta\approx$0° and $\theta\approx$180°, they must be evaluated with great precision in order for their difference to achieve numerical convergence of the much smaller S_{VH} and S_{HV}. In addition, Eqs.(40a),(40b) explain why the cross-polarized channels exhibit the TE-polarized first and second order rainbows so frequently. Since the TE-polarized S_{VV} and the TM-polarized S_{HH} are present with roughly equal magnitudes, as long as the TE-polarized rainbow with its prominent main peak dominates in S_{VV} over the TM-polarized rainbow with the main peak absent in S_{HH}, the TE rainbows will be visible in both cross-polarized amplitudes. This point will be pursued further in the context of the Debye series in [2].

5. Approximation for $\theta\approx$0° and $\theta\approx$180°

The asymptotic expansion of the associated Legendre functions used in Sec.3a is a transitional approximation valid in the range of scattering angles $0°\ll\theta\ll180°$. But it is not valid for other ranges such as $\theta\approx$0° and $\theta\approx$180°. A different transitional approximation must be employed in these other regions instead, the details of which are described in this section. The use of different approximations in different angular intervals can be avoided by using a uniform approximation which smoothly interpolates between one region of θ and another. This mathematically more elegant, but more complicated [14], approach will not be pursued here. As was mentioned in Sec.2c of [1], S_{VV}, S_{HH}, S_{VH}, and S_{HV} are individually proportional to the co-polarized and cross-polarized electric fields for $0°\ll\theta\ll180°$. But their intrinsic φ-dependence requires that they be combined together at θ=0° and θ=180° in order to eliminate that φ-dependence and generate the co-polarized and cross-polarized electric fields. The transition between these two regimes is given in this section for near-forward and near-backward scattering.

5a. Near-Forward Scattering

The GLMT angular functions $\pi_n^m(\theta)$ and $\tau_n^m(\theta)$ are well-approximated in the near-forward direction by [8]

$$m\pi_n^0(\theta) = 0 \quad \text{for } m = 0 \tag{41a}$$

$$m\pi_n^m(\theta) \approx (n+1/2)^m \, [(n+1/2)/2] \, [J_{m-1}(\Theta_n) + J_{m+1}(\Theta_n)] \quad \text{for } m \geq 1 \tag{41b}$$

$$\tau_n^0(\theta) \approx -(n+1/2)\, J_1(\Theta_n) \quad \text{for } m = 0 \tag{41c}$$

$$\tau_n^m(\theta) \approx (n+1/2)^m \, [(n+1/2)/2] \, [J_{m-1}(\Theta_n) - J_{m+1}(\Theta_n)] \quad \text{for } m \geq 1 \, , \tag{41d}$$

where

$$\Theta_n \equiv (n+1/2)\, \theta \, . \tag{42}$$

and $J_m(\Theta_n)$ is a Bessel function. When this approximation to the GLMT angular functions is substituted into Eqs.(4a),(4b) for S_1 and S_2, the factor of $(n+1/2)^m$ in the angular function approximation again cancels the factor of $[1/(n+1/2)]^m$ in Eqs.(4a),(4b). For $\theta \approx 0°$, the unit vectors $\mathbf{u_\theta}$ and $\mathbf{u_\varphi}$ become

$$\mathbf{u_\theta} \approx \cos(\varphi)\, \mathbf{u_x} + \sin(\varphi)\, \mathbf{u_y} \tag{43a}$$

$$\mathbf{u_\varphi} \approx -\sin(\varphi)\, \mathbf{u_x} + \cos(\varphi)\, \mathbf{u_y} \, . \tag{43b}$$

The far-zone scattered electric field of Eq.(2a) then becomes

$$\mathbf{E}_{\mathbf{scatt}}(r,\theta,\varphi;\rho_0,\varphi_0) \approx [iE_0/(kr)] \exp(ikr) \{[S_2(\theta,\varphi;\rho_0,\varphi_0) \cos(\varphi) + S_1(\theta,\varphi;\rho_0,\varphi_0) \sin(\varphi)] \mathbf{u}_x + [S_2(\theta,\varphi;\rho_0,\varphi_0) \sin(\varphi) - S_1(\theta,\varphi;\rho_0,\varphi_0) \cos(\varphi)] \mathbf{u}_y\} \quad . \qquad (44)$$

The approximate GLMT angular functions of Eqs.(41a)-(41d) are substituted into the scattering amplitudes of Eqs.(4a),(4b), and the result into Eq.(44). At this point one encounters three sums over m that can be exactly analytically evaluated using the Neumann addition theorem for Bessel functions (see pp.358-359 of [15]) and the Graf addition theorem for Bessel functions (see pp.359-361 of [15]), extended to modified Bessel functions

$$J_0(A_n) = J_0(\Theta_n)\, I_0(Q_n) + 2 \sum_{m=1}^{\infty} (-i)^m J_m(\Theta_n)\, I_m(Q_n) \cos(m\chi) \qquad (45a)$$

$$- X\, J_2(A_n) = J_0(\Theta_n)\, I_2(Q_n) + \sum_{m=1}^{\infty} (-i)^m J_m(\Theta_n) [I_{m-2}(Q_n) + I_{m+2}(Q_n)] \cos(m\chi) \qquad (45b)$$

$$Y\, J_2(A_n) = \sum_{m=1}^{\infty} (-i)^m J_m(\Theta_n) [I_{m-2}(Q_n) - I_{m+2}(Q_n)] \sin(m\chi), \qquad (45c)$$

where

$$A_n \equiv (n+1/2) [\theta^2 - \varepsilon^2 + 2i\, \theta\varepsilon \cos(\chi)]^{1/2} \qquad (46a)$$

$$X = [\theta^2 \cos(2\chi) - \varepsilon^2 + 2i\, \theta\varepsilon \cos(\chi)] / [\theta^2 - \varepsilon^2 + 2i\, \theta\varepsilon \cos(\chi)] \qquad (46b)$$

$$Y = - [\theta^2 \sin(2\chi) + 2i\, \theta\varepsilon \sin(\chi)] / [\theta^2 - \varepsilon^2 + 2i\, \theta\varepsilon \cos(\chi)] , \qquad (46c)$$

with X and Y satisfying

$$X^2 + Y^2 = 1 \quad . \qquad (46d)$$

It should be noted that in Eq.(45b) when the sum of the two modified Bessel functions is replaced by their difference, and in Eq.(45c) when the difference between the two Bessel functions is replaced by their sum, the sum over azimuthal modes cannot be evaluated using the Graf addition formula. It again appears to be fortuitous that the sums over m appearing in our approximation to the scattered electric fields are those that can be evaluated analytically.

The near-forward scattered electric field for an x-polarized incident Gaussian beam with an arbitrary off-axis location is then

$$\mathbf{E}_{\mathbf{scatt}}(r,\theta,\varphi;\rho_0,\varphi_0) \approx [iE_0/(kr)] \exp(ikr) \sum_{n=1}^{\infty} F_n (n+1/2)$$

$$\times \{(a_n + b_n)\, J_0(A_n) - (a_n - b_n)\, J_2(A_n) [X \cos(2\varphi_0) + Y \sin(2\varphi_0)]\} \mathbf{u}_x$$

$$+ [iE_0/(kr)] \exp(ikr) \sum_{n=1}^{\infty} F_n (n+1/2)$$

$$\times (a_n - b_n)\, J_2(A_n)\, [Y \cos(2\varphi_0) - X \sin(2\varphi_0)]\, \mathbf{u_y} \ . \qquad (47)$$

The x component of Eq.(47) is $\mathbf{E_{VV}}$ and the y component is $\mathbf{E_{VH}}$. Similarly, for a y-polarized incident Gaussian beam with an arbitrary off-axis location, the near-forward scattered electric field is

$$\mathbf{E_{scatt}}(r,\theta,\varphi;\rho_0,\varphi_0) \approx [iE_0/(kr)] \exp(ikr) \sum_{n=1}^{\infty} F_n\, (n+1/2)$$

$$\times (a_n - b_n)\, J_2(A_n)\, [Y \cos(2\varphi_0) - X \sin(2\varphi_0)]\, \mathbf{u_x}$$

$$+ [iE_0/(kr)] \exp(ikr) \sum_{n=1}^{\infty} F_n\, (n+1/2)$$

$$\times \{(a_n + b_n)\, J_0(A_n) + (a_n - b_n)\, J_2(A_n)\, [X \cos(2\varphi_0) + Y \sin(2\varphi_0)]\}\, \mathbf{u_y} \ . \qquad (48)$$

The x component of Eq.(48) is $\mathbf{E_{HV}}$ and the y component is $\mathbf{E_{HH}}$. The terms proportional to (a_n+b_n) represent the contribution of diffraction plus the geometric processes of external reflection, transmission, etc., averaged over the TE and TM polarizations. The VV- and HH-polarized electric fields with $a_n+b_n=1$ in the context of the Debye series are of the form expected for diffraction by a circular obstacle as described in the Appendix. The terms proportional to (a_n-b_n) represent the contribution of the geometric processes of external reflection, transmission, etc., for the difference between the TE and TM polarizations. Thus diffraction does not contribute to VH and HV scattering. Equations (47),(48) for our approximations agree with the exact GLMT equations of Eqs.(22),(24) of [1] in the θ=0° limit.

5*b. Near-Backward Scattering*

The GLMT angular functions $\pi_n^m(\theta)$ and $\tau_n^m(\theta)$ are well-approximated in the near-backward direction by [8]

$$m\pi_n^0(\xi) = 0 \quad \text{for } m = 0 \qquad (49a)$$

$$m\pi_n^m(\xi) \approx (-1)^{n+m}\, (n+1/2)^m\, [(n+1/2)/2]\, [J_{m-1}(\Xi_n) + J_{m+1}(\Xi_n)] \quad \text{for } m \geq 1 \qquad (49b)$$

$$\tau_n^0(\xi) \approx (-1)^n\, (n+1/2)\, J_1(\Xi_n) \quad \text{for } m = 0 \qquad (49c)$$

$$\tau_n^m(\xi) \approx -\,(-1)^{n+m}\, (n+1/2)^m\, [(n+1/2)/2]\, [J_{m-1}(\Xi_n) - J_{m+1}(\Xi_n)] \quad \text{for } m \geq 1 \qquad (49d)$$

where

$$\xi = 180° - \theta \qquad (50a)$$

$$\Xi_n = (n+1/2)\, \xi \ . \qquad (50b)$$

When this approximation to the GLMT angular functions is substituted into Eqs.(4a),(4b), the factor of $(n+1/2)^m$ in the angular function approximation again cancels the factor of $[1/(n+1/2)]^m$ in Eqs.(4a),(4b). For $\theta \approx 180°$, the unit vectors $\mathbf{u_\theta}$ and $\mathbf{u_\varphi}$ become

$$\mathbf{u_\theta} \approx -\cos(\varphi)\, \mathbf{u_x} - \sin(\varphi)\, \mathbf{u_y} \qquad (51a)$$

$$\mathbf{u_\varphi} \approx -\sin(\varphi)\, \mathbf{u_x} + \cos(\varphi)\, \mathbf{u_y} \ . \qquad (51b)$$

The scattered electric field of Eq.(2a) then becomes

$$\mathbf{E_{scatt}}(r,\theta,\varphi;\rho_0,\varphi_0) \approx [iE_0/(kr)] \exp(ikr)\{[- S_2(\theta,\varphi;\rho_0,\varphi_0) \cos(\varphi) + S_1(\theta,\varphi;\rho_0,\varphi_0) \sin(\varphi)] \mathbf{u_x}$$

$$- [S_2(\theta,\varphi;\rho_0,\varphi_0) \sin(\varphi) + S_1(\theta,\varphi;\rho_0,\varphi_0) \cos(\varphi)] \mathbf{u}_y\} \quad . \qquad (52)$$

The approximate GLMT angular functions of Eqs.(49a)-(49d) are substituted into the scattering amplitudes of Eqs.(4a),(4b), and the result is substituted into Eq.(52). One then encounters three new sums over m which, fortunately, are the complex conjugates of Eqs.(45a)-(45c). The near-backward scattered electric field for an x-polarized incident Gaussian beam is then

$$\mathbf{E_{scatt}}(r,\theta,\varphi;\rho_0,\varphi_0) \approx [iE_0/(kr)] \exp(ikr) \sum_{n=1}^{\infty} (-1)^n F_n (n+1/2)$$

$$\times\{(a_n + b_n) J_2(A_n^*) [X^* \cos(2\varphi_0) + Y^* \sin(2\varphi_0)] - (a_n - b_n) J_0(A_n^*)\} \mathbf{u_x}$$

$$- [iE_0/(kr)] \exp(ikr) \sum_{n=1}^{\infty} (-1)^n F_n (n+1/2)$$

$$\times (a_n + b_n) J_2(A_n^*) [Y^* \cos(2\varphi_0) - X^* \sin(2\varphi_0)]\} \mathbf{u_y} \ , \qquad (53)$$

where the asterisk denotes complex conjugation. As before, the x component of Eq.(53) is $\mathbf{E_{VV}}$ and the y component is $\mathbf{E_{VH}}$. Similarly, for a y-polarized incident beam, the near-backward scattered electric field is

$$\mathbf{E_{scatt}}(r,\theta,\varphi;\rho_0,\varphi_0) \approx - [iE_0/(kr)] \exp(ikr) \sum_{n=1}^{\infty} (-1)^n F_n (n+1/2)$$

$$\times (a_n + b_n) J_2(A_n^*) [Y^* \cos(2\varphi_0) - X^* \sin(2\varphi_0)]\} \mathbf{u_x}$$

$$- [iE_0/(kr)] \exp(ikr) \sum_{n=1}^{\infty} (-1)^n F_n (n+1/2)$$

$$\times \{(a_n + b_n) J_2(A_n^*) [X^* \cos(2\varphi_0) + Y^* \sin(2\varphi_0)] + (a_n - b_n) J_0(A_n^*) \} \mathbf{u_y} \ . \quad (54)$$

The x component of Eq.(54) is $\mathbf{E_{HV}}$ and the y component is $\mathbf{E_{HH}}$. Equations (53),(54) for our approximation agree with the exact GLMT equations of Eqs.(29),(31) of [1] in the θ=180° limit.

5*c. Simplification for Incidence in the Scattering Plane*

The scattering plane is here taken as φ=±90°with $\theta \geq 0$ rather than φ=90° with θ being both positive and negative. The beam is translated with φ_0=-90° for off-axis incidence in the scattering plane. For $\theta \approx 0°$, the quantities A_n, X, and Y of Eqs.(46a)-(46c) simplify to

$$A_n = (n+1/2) (i\varepsilon \mp \theta) \qquad (55a)$$

$$X = 1 \qquad (55b)$$

$$Y = 0 \ . \qquad (55c)$$

For $\theta \approx 180°$, A_n^*, X^*, and Y^* simplify to

$$A_n^* = (n+1/2) (- i\varepsilon \mp \xi) \qquad (56a)$$

$$X^* = 1 \tag{56b}$$

$$Y^* = 0 \ . \tag{56c}$$

5d. Simplification for Incidence Perpendicular to the Scattering Plane

The scattering plane is again $\varphi=\pm 90°$ and the beam is translated with $\varphi_0=180°$ for off-axis incidence perpendicular to the scattering plane. For $\theta \approx 0°$, A_n, X, and Y simplify to

$$A_n = (n+1/2)\ (\theta^2 - \varepsilon^2)^{1/2} \tag{57a}$$

$$X = -\ (\theta^2 + \varepsilon^2\ ) / (\theta^2 - \varepsilon^2) \tag{57b}$$

$$Y = \pm\ 2\mathrm{i}\ \theta\varepsilon / (\theta^2 - \varepsilon^2)\ . \tag{57c}$$

Care is needed when evaluating the products $X\,J_2(A_n)$ and $Y\,J_2(A_n)$ at $\theta=\varepsilon$ since the both denominator of X and Y and the Bessel function $J_2(A_n)$ simultaneously vanish. The product of the two remains finite with

$$X\,J_2(A_n) = \varepsilon^2/4 \tag{58a}$$

$$Y\,J_2(A_n) = \pm\ \mathrm{i}\varepsilon^2/4\ . \tag{58b}$$

For $\theta \approx 180°$, A_n^*, X^*, and Y^* simplify to

$$A_n^* = (n+1/2)\ (\xi^2 - \varepsilon^2)^{1/2} \tag{59a}$$

$$X^* = -\ (\xi^2 + \varepsilon^2\ ) / (\xi^2 - \varepsilon^2) \tag{59b}$$

$$Y^* = \mp\ 2\mathrm{i}\ \xi\varepsilon / (\xi^2 - \varepsilon^2)\ . \tag{59c}$$

When $\xi = \varepsilon$, the potential divergence discussed above again cancels and

$$X^*\,J_2(A_n^*) = \varepsilon^2/4 \tag{60a}$$

$$Y^*\,J_2(A_n^*) = \mp\ \mathrm{i}\varepsilon^2/4\ . \tag{60b}$$

The approximation of Sec.3 was said to be valid only for the region $0°\ll\theta\ll180°$. This is the region in which the Legendre functions are oscillatory, and avoids the $\theta\approx0°$ and $\theta\approx180°$ regions where they monotonically increase as Bessel functions of suitably small arguments. Numerical computations for both in-plane scattering for $\varphi=90°$, $\varphi_0=-90°$ in Figs.1,2 and out-of-plane scattering for $\varphi=90°$, $\varphi_0=180°$ in Figs.3,4 show that the $0°\ll\theta\ll180°$ approximation of Sec.3 closely matches the exact GLMT results down $\theta\sim1°$ or less. This seemingly paradoxical result may be understood as follows. It was seen in Eqs.(47),(48) that the contribution of the n partial wave to diffraction is proportional to $J_0(A_n)$, with A_n given by Eq.(55a) for in-plane scattering and by Eq.(57a) for out-of-plane scattering. As was mentioned in Sec.4, the largest partial wave for the numerical example considered here is $n_{max}=563$. Since large partial waves near n_{max} are expected to dominate in-plane scattering, the first zero of $J_0(A_{nmax})$, which may be very qualitatively taken as a measure of the transition from the monotonic to oscillatory behavior of J_0, occurs for $\theta\sim0.24°$. For out-of-plane scattering, $J_0(A_n)$ changes from a modified Bessel function to a regular Bessel function for all partial waves when $A_n=0$, or $\theta=\varepsilon=0.92°$. Considering this change of Bessel function type to also be characteristic of the transition from monotonic to oscillatory behavior, both of these crude angular estimates are comparable to observed region of validity of the $0°\ll\theta\ll180°$ approximation of Sec.3 down to $\theta\sim1°$. A similar argument can also be made in the vicinity of back-scattering.

6. Summary

The circular symmetry of an incident plane wave or an on-axis Gaussian beam with respect to the center of a spherical particle permits the scattered electric and magnetic fields to be expressed as a sum over partial waves n. However, translating the Gaussian beam off-axis by the distance ρ_0 in the φ_0 direction breaks the circular symmetry. An inevitable consequence of this is that the scattered electric and magnetic fields must now be expressed as a double sum over partial waves n and azimuthal modes m. We have obtained a pair of transitional approximations to the GLMT scattering amplitudes $S_1(\theta,\varphi;\rho_0,\varphi_0)$ and $S_2(\theta,\varphi;\rho_0,\varphi_0)$ for which we were able to analytically evaluate all the sums over azimuthal modes in the $n\gg1$ limit, both for $\theta\approx0°$ and $\theta\approx180°$, as well as for $0°\ll\theta\ll180°$.

The key to the approximation was obtaining a series expansion of the GLMT angular functions $\tau_n^m(\theta)$ and $m\pi_n^m(\theta)$, so that each term of the series cancelled an important contribution to the m-dependence of the beam shape coefficients. Thus a number of cancellations in off-axis GLMT and which had previously occurred hidden from view in the details of numerical computations, are now allowed to take place in plain sight analytically. This provides an arguably simpler and numerically more stable set of formulas for the scattering amplitudes S_1 and S_2 in the small wavelength limit. The approximation developed here cannot be expected to be valid for all beams and all scattering particles. It is appropriate only for large particles, $2\pi a/\lambda\gg1$, and weakly focused Gaussian beams, $s\ll1$. Within this region of applicability, the approximation was found to provide a close fit to the exact GLMT results for a number of off-axis locations of the incident beam. However, only the case of $z_0=0$ was considered here. The approximation derived in this study should be extendable to all values of z_0.

It is presently uncertain as to whether the sums over azimuthal modes can be exactly evaluated analytically only for an off-axis Gaussian beam, or whether they can be exactly evaluated for more general beam types, such as an off-axis zero-order Bessel beam, for which the on-axis beam shape coefficients are known exactly [16-19]. The key to this is whether the $(n+1/2)^m$ factors in the GLMT angular functions can be either exactly or approximately cancelled away by the vector spherical harmonic translation coefficients [20-24] that are used to convert on-axis beam shape coefficients into off-axis beam shape coefficients. This topic deserves further study.

Appendix: Diffraction of an Off-Axis Gaussian Beam by a Circular Aperture

Consider a scalar Gaussian beam of constant field half-width w_0 and centered at (ρ_0,φ_0) incident on a circular aperture of radius a whose center coincides with the origin of the coordinate system. A crude model of the non-spreading beam considered in [1] is

$$E_{beam}(\rho',\varphi';\rho_0,\varphi_0) = E_0 \exp(\mathrm{i}kz) \exp[-s^2 (k\rho')^2] \exp(-\rho_0^2/w_0^2)$$
$$\times \exp[\varepsilon (k\rho') \cos(\varphi'-\varphi_0)] \quad . \qquad \text{(A1)}$$

The far-zone Fraunhofer limit of the Fresnel-Kirchhoff approximation to diffraction at the position (r,θ,φ) on the viewing screen is (see section 8.3.3 of [25])

$$E_{diffracted}(r,\theta,\varphi) = -\,\mathrm{i}k^2/(2\pi kr) \int_{\rho'=0}^{a} \rho' \,\mathrm{d}\rho' \int_{\varphi'=0}^{2\pi} \mathrm{d}\varphi' \exp[-\mathrm{i}k\rho' \sin(\theta) \cos(\varphi'-\varphi)]$$
$$\times E_{beam}(\rho',\varphi';\rho_0,\varphi_0) \quad . \qquad \text{(A2)}$$

The integral over φ' in Eq.(A2) can be evaluated analytically using the following procedure. (i) One uses $\sin(\theta) \approx \theta$ for small θ in the near-forward direction. (ii) One then expands the factor $\exp[-\mathrm{i}k\rho' \sin(\theta) \cos(\varphi'-\varphi)]$ as a Fourier series of azimuthal modes m, giving (see p.585, Eq.(11.1.4) of [3] and p.299 of [9])

$$\exp[-\mathrm{i}k\rho'\theta \cos(\varphi'-\varphi)] = \sum_{m=-\infty}^{\infty} (-\mathrm{i})^m \mathrm{J}_m(k\rho'\theta) \exp[\mathrm{i}m(\varphi'-\varphi)] \quad . \qquad \text{(A3)}$$

(iii) One then evaluates the φ' integral term-by-term using the change of variables

$$\zeta = \varphi' - \varphi \tag{A4}$$

and (see p.587, Eq.(11.1.16.b) and p.615, Eq.(11.5.14) of [3])

$$I_m(x) = (1/2\pi) \int_{\zeta=0}^{2\pi} d\zeta \exp[x \cos(\zeta)] \exp(im\zeta) \ . \tag{A5}$$

(iv) One then evaluates the m sum analytically using the Neumann addition function for Bessel functions of Eq.(45a). The diffracted field then reduces to the one-dimensional integral

$$E_{diffracted}(r,\theta,\varphi;\rho_0,\varphi_0) = [-iE_0/(kr)] \exp(ikz) \int_{k\rho'=0}^{ka} (k\rho') \, d(k\rho')$$

$$\times \exp[-s^2 (k\rho')^2] \exp(-\rho_0^2/w_0^2) \, J_0(A) \ , \tag{A6}$$

where

$$Q \equiv (k\rho') \, \varepsilon \tag{A7}$$

in analogy to Eq.(5c),

$$\Theta \equiv (k\rho') \, \theta \tag{A8}$$

in analogy to Eq.(42),

$$A = (k\rho') \, [\theta^2 - \varepsilon^2 + 2i \, \theta\varepsilon \cos(\chi)]^{1/2} \tag{A9}$$

in analogy to Eq.(46a), and

$$\chi \equiv \varphi - \varphi_0 \ . \tag{A10}$$

If one was interested instead in diffraction by a circular obstacle of radius a, Babinet's principle (see Sec.9.7 of [26]) is used to replace the leading factor of –i in Eq.(A6) by +i.

The portion of the $\mathbf{E_{VV}}$ and $\mathbf{E_{HH}}$ in the near-forward direction in Eqs.(47),(48) proportional to $J_0(A_n)$ is our approximation to diffraction of an off-axis Gaussian beam by a spherical particle for the Debye series assignment (see pp.209-210 of [9] and [27]) $a_n = b_n = 1/2$. Using van de Hulst's localization principle (see pp.208-209 of [9]) in Eq.(A6) to approximately convert the integral over the impact parameter $k\rho'$ into a sum over partial waves n via $k\rho' \rightarrow (n+1/2)$, the result of Eq.(A6) is identical to the circular obstacle diffraction pattern of Eqs.(47),(48). The analysis of Eq.(A6) will be given in [2].

Acknowledgement

J.A.L. and P.L. thank Prof. David Cannell of the University of California at Santa Barbara for a series of conversations that led to our investigation of cross-polarized scattering.

References

[1] Lock JA., Laven P, Co-polarized and cross-polarized scattering of an off-axis focused Gaussian beam by a spherical particle. 1. Exact GLMT formalism. JQSRT 2018; 221, 260-272.

[2] Laven P, Lock JA. Co-polarized and cross-polarized scattering of an off-axis focused Gaussian beam by a spherical particle. 3. Diffraction, the Debye series and time domain scattering. JQSRT 2018; 221, 286-299.

[3] Arfken G. Mathematical methods for physicists, third ed. Orlando FL:Academic;1985.

[4] Gradshteyn IS, Ryzhik IM. Table of Integrals, Series, and Products, seventh ed. Amsterdam:Academic;2007.

[5] Abramowitz M, Stegun IA. Handbook of mathematical functions. Washington D.C.:Nat Bureau Standards;1964.

[6] van de Hulst HC. Optics of spherical particles. Recherches Astronomique de l'Observatoire d'Utrecht 1946;XI;1-87.

[7] Jahnke E, Emde F. Tables of functions, fourth edition. New York:Dover;1945.

[8] Lock JA. Contribution of high-order rainbows to the scattering of a Gaussian laser beam by a spherical particle. J Opt Soc Am A 1993;10:693-706.

[9] van de Hulst HC. Light Scattering by Small Particles. New York:Dover;1981.

[10] Wiscombe WJ. Improved Mie scattering algorithms. Appl Opt 1980;19:1505-9.

[11] Lock J, Laven P. The Debye series and its use in time-domain scattering, in Kokhanovsky A. ed. Light Scattering Reviews 11. Springer Praxis:Berlin;2016.

[12] Shen J, Liu X, Wang W, Yu H. Calculation of light scattering of an elliptical Gaussian beam by a spherical particle. J Opt Soc Am A 2018;35:1288-98.

[13] Laven P. Scattering of Gaussian beams by a spherical particle. http://www.philiplaven.com/p3d2.html.

[14] Nussenzveig HM. High-frequency scattering by an impenetrable sphere. Ann Phys (NY) 1965;34:23-95. Eq.(C11).

[15] Watson GN. A treatise on the theory of Bessel functions, 2nd ed. Cambridge UK: Cambridge University Press;1958.

[16] Mishra SR. A vector wave analysis of a Bessel beam. Opt Comm 1991; 85: 159-61.

[17] Lock JA. Angular spectrum and localized model of Davis-type beam. J Opt Soc Am A 2013; 30: 489-500.

[18] Wang JJ, Wriedt T, Lock JA, Madler L. General description of circularly symmetric Bessel beams of arbitrary order. JQSRT 2016;184:218-32.

[19] Mitri FG, Li RX, Yang RP, Guo LX, Ding CY. Optical pulling force on a magneto-dielectric Rayleigh sphere in Bessel tractor polarized beams. JQSRT 2016;84:360-81.

[20] Friedman B, Russek J. Addition theorems for spherical waves. Quart Appl Math 1954;12:13-23.

[21] Stein S. Addition theorems for spherical wave functions. Quart Appl Math 1961;19:15-24.

[22] Cruzan OR. Translation addition theorems for spherical vector wave functions. Quart Appl Math 1962;20:33-40.

[23] Dociu A, Wriedt T. Plane wave spectrum of electromagnetic beams. Opt Comm 1997;136:114-24.

[24] Boyde L, Chalut KJ, Guck J. Exact analytical expansion of an off-axis Gaussian laser beam using the translation theorems for the vector spherical harmonics. Appl Opt 2011;50:1023-33.

[25] Born M, Wolf E. Principles of Optics, 7th edition. Cambridge UK: Cambridge University Press;1999.

[26] Jackson JD. Classical electrodynamics, 1st ed. New York: Wiley; 1962.

[27] Lock JA. Diffraction of a Gaussian beam by a spherical obstacle. Am Journ Phys 1993;61:698-707.